Comparative Study of Temporomandibular Articular Fossa Bone Surface and the Envelope Surface of the Condyle Movement

Ke Nan CHEN[1#], Jing WANG[1#], Jun Peng CHEN[1], Jun Lin WANG[1], Yu Chun SUN[2], Xiang Liang XU[1], Chuan Bin GUO[1]

Objective: *To investigate the differences between temporomandibular articular fossa bone surface and the envelope surface of the mandibular condyle movement.*

Methods: *Thirty-four healthy adults underwent skull base and mandible scans using CBCT and performed mandibular border movement using the mandibular movement recording system. Landmarks of the fossa and tubercle were indicated and distance and angle parameters were measured on the 3D models reconstructed from the CBCT. The condyle movement envelope surfaces were formed according to models reconstructed from CBCT and the mandibular movement trajectory using computer simulation. The highest and lowest points of the envelope surface were indicated to create parameters. The data were analysed using a paired t test in SPSS (version 24.0, IBM, Armonk, NY, USA).*

Results: *The mandibular fossa bone surface was statistically different to the envelope surface for the height of the first peak of the envelope surface (3.280 ± 1.319 mm) and depth of the mandibular fossa (6.338 ± 2.389 mm) (the ratio was 51.75%), the height of the second peak of the envelope surface (1.463 ± 0.745 mm) and the height of the tubercle (2.000 ± 0.968 mm) (the ratio was 73.15%), and the downwards angle of the envelope surface (25.933 ± 7.539 degrees) and the posterior slope angle of the articular tubercle (35.059 ± 5.224 degrees) (the ratio was 73.97%).*

Conclusion: *The downwards angle of the envelope surface was statistically significantly smaller than the posterior slope angle of the articular tubercle, suggesting that the condyle movement is flatter than the mandibular fossa bone surface.*

Key words: *artificial fossa component, condyle movement, envelope surface, mandibular fossa bone surface, temporomandibular joint*

Chin J Dent Res 2022;25(3):179–187; doi: 10.3290/j.cjdr.b3317993

1 Department of Oral and Maxillofacial Surgery, Peking University School and Hospital of Stomatology, National Centre of Stomatology, National Clinical Research Centre for Oral Diseases, National Engineering Research Centre of Oral Biomaterials and Digital Medical Devices, Beijing Key Laboratory of Digital Stomatology, Research Centre of Engineering and Technology for Computerised Dentistry, Ministry of Health, NMPA Key Laboratory for Dental Materials, Beijing, P.R. China.

2 Centre of Digital Dentistry, Peking University School and Hospital of Stomatology, Beijing, P.R. China.

\# These two authors contributed equally to this work.

Corresponding authors: Prof Chuan Bin GUO and Associate Prof Xiang Liang XU, Department of Oral and Maxillofacial Surgery, Peking University School and Hospital of Stomatology, #22 Zhongguancun South Avenue, Haidian District, Beijing, 100081, P.R. China. Tel: 86-10-82195398; Fax: 86-10-82195710. Email: guodazuo@sina.com; kqxxl@126.com

This work was supported by grants from the Beijing Municipal Science and Technology Commission (grant number Z201100005520055) and the National Key R&D Programme of China (grant number 2019YFB1706900).

The temporomandibular joint (TMJ) is one of the most complex joints in the human body and plays an important role in the functions of chewing, swallowing and speaking[1-4]. Although the TMJ is comprised of only two bones, McKay et al[5] consider it as a double joint because the articular disc covers the condyle and interposes below the fossa, dividing the joint cavity into superior and inferior compartments. The movement of the TMJ is usually divided into translation and rotation: the upper compartment, the discotemporal compartment, in which the condyle–disc complex translates on the posterior slope of the articular eminence, and the lower compartment, the discomandibular compartment, in which the mandibular condyle rotates on the lower aspect of the articular disc[6]. The superior portion of the disc is in contact with the posterior surface of the articular tubercle, with the function of preventing the disc from slipping during mouth opening. The inferior portion has the task of avoiding excessive rotational movements of the disk relative to the mandibular condyle[1].

The morphology of the TMJ[7,8] and research about movement of the condyle have been well documented in some studies[2,4,9,10]. As the condyle moves out of centric relation, it descends along the posterior slope of the articular eminence of the mandibular fossa[11]. From an anatomical perspective, the articular facet of the TMJ includes the mandibular fossa and anterior articular tubercle; however, from a functional perspective, the anterior boundary of the TMJ is the front end of the anterior slope of the articular tubercle, where the border movement of the condyle can reach. The TMJ facet is the posterior aspect of the articular eminence (articular slope), the anterior slope of the mandibular condyle and the anterior segment (anterior to the Glaser fissure) of the mandibular fossa. It has been proposed that sagittal guidance of the condyle is related to the height and slope of the posterior surface of the articular tubercle[11]. As cited in Singh et al[11], glossary of prosthodontic terms defines condylar guidance as “mandibular guidance generated by the condyle and articular disc traversing the contour of the glenoid fossae". Considering the articular discs and the bone cartilage between the condyle and fossa bone are flexible and prone to deformation when mastication or movement causes compression, there should be a difference between the path of condylar movement and the posterior slope of the articular tubercle.

Based on the anatomical structures of the TMJ and the relevant literature, it is hypothesised that the shape of the envelope surface is not significantly different from the mandibular fossa bone surface. Few articles have investigated the difference between condyle movement and mandibular fossa bone surface quantitatively. One important reason for this is that movement data for the TMJ cannot be obtained directly. Most of the previous studies on the movement of the mandibular condylar process obtained the movement trajectory of the condylar process through landmark points, but this method did not accurately reflect the 3D movement shape of the condylar process[12,13]. In a previous study by the present authors, the 3D envelope surface of the condylar process movement was investigated and the concept of the condyle movement functional surface was identified, including a 3D motion range of the condylar process[14]. The condylar movement envelope surface is a fusion of condylar digital models at different positions during mandibular movement that represents the 3D boundary range that the condylar process can reach. The condylar envelope surface can be measured quantitatively so that information on condylar movement can be obtained by measuring the envelope surface. In addition, by measuring it quantitatively, information on biological condyle movement can be obtained. The envelope surface of condylar movement recorded from normal adults could be applied when designing an artificial joint replacement system with the help of 3D printing technology, resulting in a more physiological design of the artificial TMJ.

The present study aims to preliminarily explore a quantitative method for measuring the envelope surface of condylar process movement and compare it with the mandibular fossa bone surface. This study provides a reliable data basis for the above hypothesis and more information on the movement of the condyle in the physiological state.

Materials and methods

Subjects

This study was approved by the Bioethics Committee of Peking University School and Hospital of Stomatology, Beijing, China (no. Pkussirb-201947091). Twenty-five women (aged 26.22 ± 1.922 years) and nine men (aged 25.48 ± 2.95 years) were selected according to the following inclusion criteria:

- no systemic disease;
- facial symmetry;
- no history of maxillofacial trauma or surgery;
- no history of orthodontic treatment;
- no TMJ discomfort, such as pain, clicking, limited mouth opening or any history of TMJ treatment;
- no abnormal habits, such as bruxism or clenching;

Table 1 Landmarks and parameters of the articular fossa bone surface.

Landmarks and parameters	Abbreviation	Definition
Orbitale	O	Lowest point on the lower edge of the cranial orbit
Porion	P	Highest point on the external auditory canal
Frankfurt horizontal plane	FH plane	Determined by left porion, right porion and the midpoint of orbitales
Fossa	F	Highest point of the articular fossa
Tubercle	T	Lowest point of the articular tubercle
Starting point of the articular tubercle	Ta	Anterior starting point of the articular tubercle
Posterior slope angle of the articular tubercle	Angle α	Angle between the line passing through point F and point T and the FH plane
Anterior slope angle of the articular tubercle	Angle β	Angle between the line passing through point T and point Ta and the FH plane
Fossa depth	$Y_{F\text{-}T}$	Distance between point F and point T in Y-axis direction
Tubercle height	$Y_{T\text{-}Ta}$	Distance between point T and point Ta in Y-axis direction

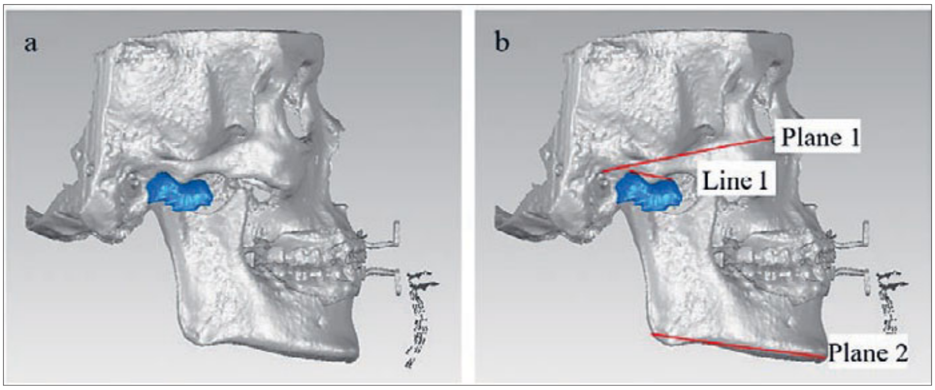

Fig 1 **(a)** Registration model and acquisition of the envelope surface (blue part). **(b)** The FH plane (plane 1), the mandibular body plane (plane 2) and the line connecting the two peaks of the envelope surface (line 1), the mandibular body angle and the MBP-ES angle (the angle between the envelope surface and the mandibular body plane) can be obtained; the angle between FH plane and line 1 can be calculated.

- full dentition and a Class I occlusal relationship.

Each volunteer underwent a clinical examination to assess TMJ function, occlusion and facial form. The examination was carried out by three trained professional doctors separately and assessed whether the TMJ experienced clicking, pain or an opening restriction, as well as no obvious deviation and abnormality of the mandibular movement during opening. Informed consent was obtained from all participants.

Imaging data collection

All volunteers underwent skull base and mandible CBCT scans (NewTom VG, NewTom, Imola, Italy; voxel size 0.3 mm, field of view 16 cm × 16 cm) at the intercuspal position (ICP) to obtain DICOM data. The CBCT was imported into ProPlan CMF 3.0 (Materialise, Leuven, Belgium) in DICOM format. Separation of the maxilla and mandible was achieved by selecting the appropriate bone tissue threshold in the software, and the reconstructed maxilla and mandible were exported in stereolithography (STL) format.

Parameters of the mandibular fossa bone surface

The CBCT of the ICP was imported into ProPlan CMF 3.0 in DICOM format to measure the parameters of the mandibular fossa bone surface. The landmarks of the articular facet were indicated and the direction was defined as perpendicular to the Frankfurt horizontal plane (FH plane) as the Y-axis. The distances from the indicated points and FH plane, the posterior slope of the articular tubercle (angle α) and the anterior slope of the articular tubercle (angle β) could be measured directly and fossa depth (distance between point F and point T in the Y-axis direction, $Y_{F\text{-}T}$) and tubercle height (distance between point T and point Ta in Y-axis direction, $Y_{T\text{-}Ta}$) can be calculated as shown in Table 1 and Fig 1.

3D splint printing

The 3D morphological data and relative position in intercuspal occlusion of the maxillary and mandibular dentition of volunteers were obtained using a TRIOS 3 intraoral scanner (3Shape, Copenhagen, Denmark) in the ICP. Two splints were created to attach the maxillary and mandibular eight anterior teeth in Geomagic Studio

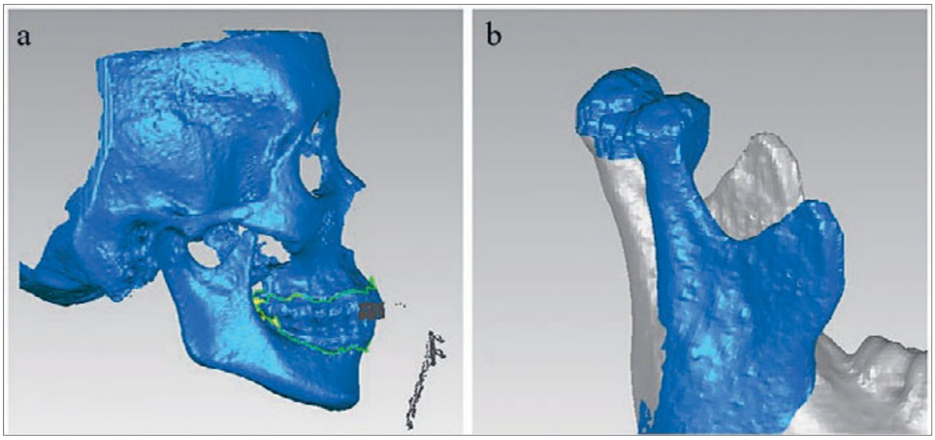

Fig 2 **(a)** Registration models. **(b)** The positions of the condyle at each moment were saved in the same 3D coordinated system merged to construct the envelope surface.

(3D Systems, Rock Hill, SC, USA) using the scanned dentition model. The splints were obtained using a 3D printer (SHINO I, SHINO, Beijing, China; nozzle diameter 0.3 mm, thickness 0.1 mm).

Mandibular movement trajectory collection

Volunteers performed border movements with a splint on their teeth with landmarks stuck to it. The movement trajectory of the target was measured at 120 HZ using the mandibular movement recording system PN300 (GeoVision, Taipei, Taiwan) and the result was represented by the coordinate points in the coordinate system. The core binocular vision device in the PN300 system was two digital cameras. Movement information data saved in a TXT file were opened in Geomagic Studio 2012, creating a point cloud of the maxillary dentition and mandibular trajectory. The curve present in the 3D coordinated system was obtained by connecting the coordinate points resulting from the movement trajectory of the mandibular movement. The coordinated point and 3D curve were imported into Geomagic Studio 2012 and transformed into STL format. The error in the 3D real-time, computerised, binocular, tracking system was 0.1 mm[15].

Obtaining the envelope surface

The models of the skull, mandible and mandibular movement trajectories were registered in Geomagic Studio, as shown in Fig 2a. The mandibular movement was simulated according to the collected trajectory and the positions of the condyle at each moment were saved in the same 3D coordinated system. They were imported into Geomagic Studio in PLY format and merged to construct the envelope surface, as shown in Fig 2b.

Processing of the models

The envelope surface and maxillary and mandibular models were imported into Geomagic Studio in STL format in the same coordinated system, as shown in Fig 1a. The FH plane and Y-axis were the same as the models in ProPlan CMF. The mandibular body angle was defined as the angle between the FH plane and the mandibular body plane, as shown in Fig 1b. The angle between the mandibular body plane and the line crossing two peaks of the envelope surface (MBP-ES angle) can be measured directly. The angle between the line crossing two peaks of the envelope surface and the FH plane can be calculated from the MBP-ES angle and mandibular body angle. The calculation method involved comparing the mandibular body plane with the line crossing two peaks; when the mandibular body plane is flatter, it equals mandibular body angle plus MBP-ES angle; when the mandibular plane is steeper, it equals mandibular body angle minus MBP-ES angle. The landmarks of the envelope surface were indicated and parameters were measured and calculated as shown in Table 2 and Fig 3.

Results

Shape of the envelope surface

All the envelope surfaces showed a ‘two-peak’ shape. The second peak was lower than the first, and the depression between the two peaks was roughly below the

Table 2 Landmarks and parameters of the envelope surface.

Landmarks and parameters	Abbreviation	Definition
Condylion at ICP	F1	Highest point of the first peak
Lowest point of the envelope surface	T1	Lowest point between two peaks
Condylion of end position	Ta1	Highest point of the second peak
Height of first peak	$Y_{F1\text{-}T1}$	Distance between point F1 and T1 in the y-axis direction
Height of second peak	$Y_{T1\text{-}Ta1}$	Distance between point T1 and Ta1 in the y-axis direction
Downwards angle of the envelope surface	Angle α_1	Angle between the line F1-T1 and FH plane
Upwards angle of the envelope surface	Angle β_1	Angle between the line T1-Ta1 and FH plane

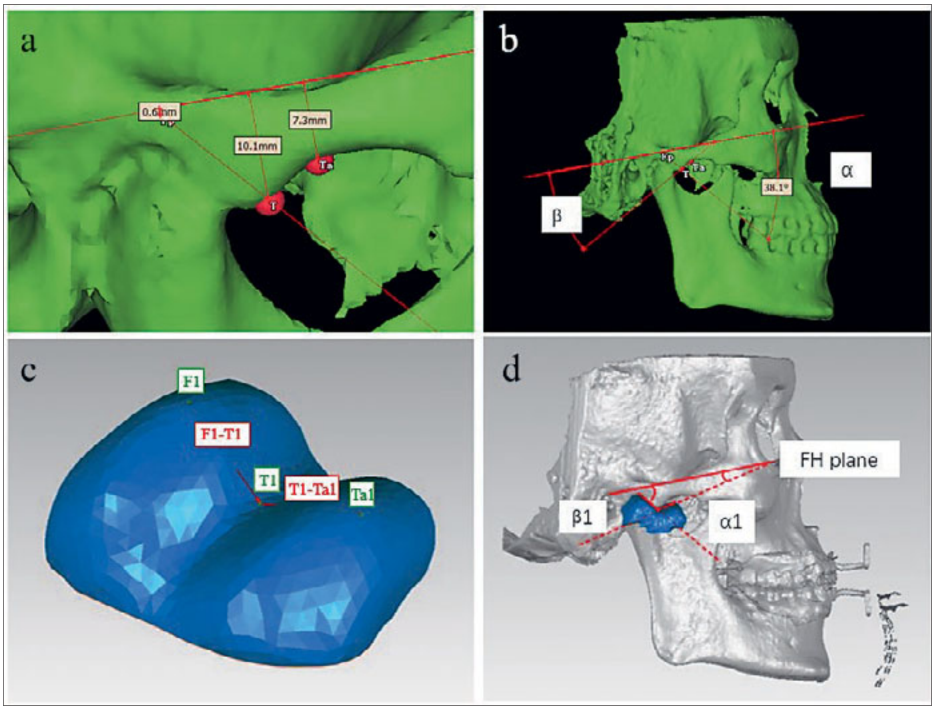

Fig 3 Landmarks of the articular fossa bone surface **(a)** and envelope surface **(c)**; angles of the articular fossa bone surface **(b)** and envelope surface **(d)**. F, highest point of the articular fossa; T, lowest point of the articular tubercle; Ta, the anterior starting point of the articular tubercle; angle α, posterior slope angle of the articular tubercle; angle β, anterior slope angle of the articular tubercle; F1, highest point of the first peak; T1, lowest point between two peaks; Ta1, highest point of the second peak; angle α_1, downwards angle of the envelope surface; angle β_1, upwards angle of the envelope surface.

articular tubercle in the registration model. The condyle moves forwards and downwards from the ICP forming the first peak and downwards surface, then crosses the lowest point of the articular tubercle and moves upwards slightly, forming the upwards surface and the second peak of the envelope surface[4].

Data analysis

The results of the measurement of the above parameters are shown in Table 3. A paired *t* test analysis was performed, the results of which are shown in Table 4 and Fig 4.

Parameters of the mandibular fossa bone surface of the TMJ and the envelope surface were measured and analysed. A paired *t* test was performed between parameters of the mandibular fossa bone surface and the envelope surface. The statistical results showed that angle α and angle α_1, $Y_{F\text{-}T}$ and $Y_{F1\text{-}T1}$, $Y_{T\text{-}Ta}$ and $Y_{T1\text{-}Ta1}$ were statistically different with $P = 0.000$, $P = 0.000$ and $P = 0.007$, respectively, which indicated significant differences between the envelope surface and the articular facet in angle α and angle α_1, as well as the vertical distances. There was no statistical difference between angle β and angle β_1. Statistically different parameters were further subjected to the following ratio calculations: angle α_1 / angle α = 73.97%, $Y_{F\text{-}T}$ / $Y_{F1\text{-}T1}$ = 51.75%, $Y_{T\text{-}Ta}$ / $Y_{T1\text{-}Ta1}$ = 73.15%. The ratio illustrated that the condyle moved half of the fossa depth in vertical distance. Angle α_1 was 10 degrees smaller than angle α, which is nearly 30% smaller than the angle of the mandibular fossa bone surface.

Discussion

The articular facet of the TMJ includes the mandibular fossa and articular tubercle. Corbett et al[16] and Mack[17] found that the condyle followed the surface of the man-

Table 3 Data analysis of the articular fossa bone surface of the TMJ and the envelope surface.

Parameters	Min	Max	Mean ± SD
Angle α, degrees	23.40	45.30	35.059 ± 5.224
Angle β, degrees	1.00	28.30	14.277 ± 6.679
$Y_{F\text{-}T}$, mm	2.70	10.90	6.338 ± 2.389
$Y_{T\text{-}Ta}$, mm	0.10	3.80	2.000 ± 0.968
Angle α_l, degrees	11.12	41.84	25.933 ± 7.539
Angle β_l, degrees	1.98	29.56	15.192 ± 6.178
$Y_{Fl\text{-}Tl}$, mm	1.21	6.51	3.280 ± 1.319
$Y_{Tl\text{-}Tal}$, mm	0.23	3.89	1.463 ± 0.745

Table 4 Paired *t* test between the parameters of the articular facet and envelope surface.

Parameters	Mean ± SD	t	*P* value
Angle α_1, degrees	25.933 ± 7.539	5.582	0.000
Angle α, degrees	35.059 ± 5.224		
Angle β_1, degrees	15.192 ± 6.178	−0.722	0.475
Angle β, degrees	14.277 ± 6.679		
$Y_{F1\text{-}T1}$, mm	3.280 ± 1.319	6.395	0.000
$Y_{F\text{-}T}$, mm	6.338 ± 2.389		
$Y_{T1\text{-}Ta1}$, mm	1.463 ± 0.745	2.869	0.007
$Y_{T\text{-}Ta}$, mm	2.000 ± 0.968		

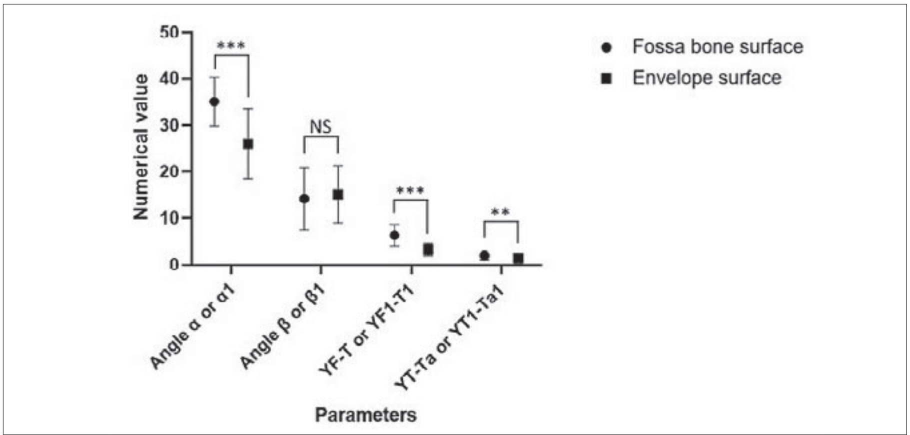

Fig 4 Parameters of the articular facet and envelope surface. $^{**}P < 0.01$, $^{***}P < 0.001$. NS, not significant

dibular fossa closely during mandibular movement. It has been proposed that sagittal condylar guidance coincides more or less with the posterior slope of the articular tubercle[11]; however, the physiological movement of the TMJ is also affected by the shape and deformation of the articular disc, restrictions of capsule and ligament, traction of muscles and other factors[17]. A more accurate assessment is as follows: the condylar path is determined by the bony fossa, the muscles responsible for mandibular movements and their nerve controls, the occlusal relationship, the shape and movements of the disc and the limitations of ligaments[11]. Theoretically, the condyle movement is related to the mandibular fossa bone surface but not completely consistent. The differences between the fossa and the condyle movement path are rarely studied. In the present study, these parameters were measured and compared statistically.

The morphology of the TMJ has been measured with different landmarks and parameters[7,8]. Common parameters of the mandibular fossa bone surface include the diameter and angle of the fossa and the height of the articular tubercle. In the present study, several sagittal landmarks and related parameters closely related to the movement of the condyle were selected. All the envelope surfaces exhibited a ‘two-peak’ shape. The second peak was lower than the first, and the depression between the two was roughly below the articular tubercle in the registration model. The highest point of the mandibular fossa (F) corresponds to the condylion in the centric relation position (F1), which is also the first peak’s highest point of the envelope surface. The downwards angle of the envelope surface (angle α_1) is formed by the forwards and downwards movement of the condyle in the guidance of the posterior slope of the articular tubercle (angle α) anatomically. The condyle then moves across the lowest point of the articular tubercle (T) and upwards a little until it reaches the maximum opening point, resulting in the formation of the second peak. Thus, the lowest point of the envelope surface (T1) corresponds to point T. Fossa depth, articular tubercle height, the posterior slope of the articular tubercle and the anterior slope of the articular tubercle were measured through points F, T and Ta. The results for fossa depth are consistent with previous studies[7,8]. The definition of tubercle height in the present study is different from that given in the previous literature because the FH plane was set as the reference plane for the measurement of the envelope surface and articular facet to make the parameters comparable. The angle α measured in this study was relatively consistent with the results of the previous literature[18].

The method of using landmark points to study the condylar process or mandibular movement has become more accurate as instruments have developed; however, the difference in the selection of landmark points causes differences in the results of the movement trajectory[12,13], and this method cannot reflect the influence of the 3D shape of the condylar process on movement trajectory. Koolstra et al[19] first introduced the concept of the envelope surface of the incisors and studied the incisor movement with the aim of evaluating the influence of the temporomandibular ligaments and the passive tension muscles on the envelope surface. Later, Huang et al[14] took the 3D shape of the condyle into consideration and analysed the 3D shape of the movement of the functional surface of the mandibular condyle. They found that the condylar movement envelope surface was the reachable range of the condylar process during mandibular border movement[14]. Thirty-four healthy adults were included in the present study and the obtained envelope surfaces presented a 'two-peak' shape, which is consistent with Huang et al[14] and may be influenced by the morphology of the articular tubercle. The first peak of the envelope surface is formed when the condyle is in the centric position as the condyle moves forwards and downwards, crosses the lowest point of the articular tubercle and then moves upwards slightly[4], forming the second peak of the envelope surface.

Results of measurements for parameters of the mandibular fossa bone surface of the TMJ and the envelope surface in this study quantitatively verified our hypothesis that the shape of the envelope surface is not significantly different from the mandibular fossa bone surface. Paired *t* test results and mean values showed that the parameters of the envelope surface are significantly smaller than the mandibular fossa bone surface, with a ratio between 50% and 75%. The data showed significant differences between the envelope surface and the articular facet with the vertical distance of the condyle moving only 51% of the fossa depth. The downwards angle of the envelope surface was 10 degrees smaller than the posterior slope angle of the articular tubercle, which is nearly 30% smaller than the mandibular fossa.

These results indicate that the tissue between the condyle and the mandibular fossa has a very important influence on the movement of the condyle. During the forwards and downwards movement of the condyle, the posterior slope of the articular tubercle still played a guiding role; however, the articular disc and other flexible tissues influenced the shape of the upper functional surface of the condyle movement, resulting in smaller downwards angles of the envelope surface than the bony slope angles of the mandibular fossa. This difference reflected the cushioning function of the structures between the mandibular fossa bone surface and the condyle process. The mismatches between the mandibular fossa and the mandibular condyle are mitigated by the articular disc, which also has the role of ensuring the congruence of the articular surfaces. The result between angle β and angle β_l was not significantly different ($P = 0.475 > 0.05$). From a physiological and anatomical perspective, this part of the bone structure had little effect on the movement of the condyle because the condyle could not reach the anterior starting point of the tubercle in the physiological status.

At present, the design of an artificial TMJ replacement system, consisting of two rigid prosthetic components, rarely includes reconstruction of the articular disc and other tissues[20]. The present results indicated that the articular disc played a highly important role in the process of condyle movement, which affected the design of the artificial TMJ. The mandibular fossa bone surface cannot replicate the envelope surface of condyle movement in the physiological status[21]. Given that the TMJR system could not replicate the reconstruction and simulation of soft tissues, such as the joint disc, at this stage, it is important to consider how the TMJR system mimics the movement of a healthy TMJ. The results of clinical trials of the TMJ system by Yang's team[22] which was designed based on the bony shape of healthy Chinese adults also suggested that artificial joints that conform to anatomical shapes still cannot still simulate the movement of a healthy TMJ[23]. Although a finite element analysis study of a custom-made temporal component that fitted the mandibular fossa bone surface showed that the geometry of the fossa promoted better load transfer of the condyle distally, this study mentioned that the design according to the fossa surface did not correspond to joint physiological movements[24].

Based on the current design of the TMJR system and the present results, it is suggested that the mandibular fossa should act as a guide for the movement of the artificial joint head. Previous studies pointed out that the 3D morphology of condylar movement could be used for the design of an artificial TMJ fossa[14,25]. Xu et al[25] designed a TMJ prosthesis that obtained the condylar movement surface of a canine as the articular surface of the fossa component, with a good result for strain distribution in the finite element analysis. The artificial TMJR system, based on the design of the condyle movement envelope surface, is more suitable for the rigid artificial prosthesis design without flexible tissue repair, such as the joint disc, at present. The purpose of the envelope surface is to provide a theoretical basis for the functional surface of the artificial joint fossa. It is hoped that the movement of the artificial joint head can be guided and supported by the reconstructed condyle movement envelope surface after the removal of the articular disc to achieve physiological mandibular movement.

Conclusion

The downwards angle of the envelope surface was statistically significantly smaller than the posterior slope angle of the articular tubercle, suggesting that the condyle movement is gentler than the mandibular fossa bone surface of the TMJ. The envelope surface of condylar movement could be helpful for the geometrical design of the fossa component in an artificial TMJR system, which may play a role in guiding the movement of the condyle component in a manner similar to that of a healthy joint.

Conflicts of interest

The authors declare no conflicts of interest related to this study.

Author contribution

Drs Ke Nan CHEN and Jing WANG conceived and designed the study, contributed to the data acquisition, analysis and interpretation and drafted the manuscript, and contributed equally to this article; Drs Jun Peng CHEN, Jun Lin WANG and Jun Qi JIANG contributed to the data collection; Dr Yu Chun SUN provided devices for the experiment; Dr Xiang Liang XU and Prof Chuan Bin GUO critically revised the manuscript for important intellectual content and gave final approval, and contributed equally to this article.

(Received Apr 24, 2022; accepted Jun 20, 2022)

References

1. Bordoni B, Varacallo M. Anatomy, Head and Neck, Temporomandibular Joint. StatPearls. Treasure Island (FL): StatPearls Publishing; 2022.
2. Krohn S, Joseph AA, Voit D, et al. Multi-slice real-time MRI of temporomandibular joint dynamics. Dentomaxillofac Radiology. 2019;48:20180162.
3. Tubbs RS, Shoja MM, Loukas M. Temporomandibular Joint. Bergman's Comprehensive Encyclopedia of Human Anatomic Variation. Hoboken: John Wiley and Sons, 2016.
4. Chen CC, Lin CC, Hsieh HP, Fu YC, Chen YJ, Lu TW. In vivo three-dimensional mandibular kinematics and functional point trajectories during temporomandibular activities using 3d fluoroscopy. Dentomaxillofac Radiol 2021;50:20190464.
5. McKay GS, Yemm R, Cadden SW. The structure and function of the temporomandibular joint. Br Dent J 1992;173:127–132.
6. Chang CL, Wang DH, Yang MC, Hsu WE, Hsu ML. Functional disorders of the temporomandibular joints: Internal derangement of the temporomandibular joint. Kaohsiung J Med Sci 2018;34:223–230.
7. Zhang LZ, Meng SS, He DM, et al. Three-dimensional measurement and cluster analysis for determining the size ranges of Chinese temporomandibular joint replacement prosthesis. Medicine (Baltimore) 2016;95:e2897.
8. Zhong Z, Sun J, Yu Z, Han Y, Kang C. Morphological study of safe fixation region of temporomandibular joint prosthesis in Chinese northeast population with 3-dimensional computed tomographic image. Medicine (Baltimore) 2020;99:e22779.
9. Krohn S, Frahm J, Mahler A, et al. Biomechanical analysis of temporomandibular joint dynamics based on real-time magnetic resonance imaging. Int J Comput Dent 2020;23:235–244.
10. Gallo LM. Modeling of temporomandibular joint function using MRI and jaw-tracking technologies--Mechanics. Cells Tissues Organs 2005;180:54–68.
11. Singh S, Das S, Bhattacharyya J, Ghosh S, Goel P, Dutta K. A comparative study to correlate between clinically and radiographically determined sagittal condylar guidance in participants with different skeletal relationships. J Indian Prosthodont Soc 2017;17:175–182.
12. Ueda K. Three-dimensional analysis for prediction and assessment of mandibular movement in orthognathic surgery in the ramus. J Maxillofac Surg 1983;11:216–226.
13. Zwijnenburg A, Megens CC, Naeije M. Influence of choice of reference point on the condylar movement paths during mandibular movements. J Oral Rehabil 1996;23:832–837.
14. Huang C, Xu XL, Li LL, Sun YC, Guo CB. A study on reconstruction of the four-dimensional movement model and envelope surface of condyle in normal adults [epub ahead of print 2 September 2021]. Br J Oral Maxillofac Surg doi: 10.1016/j.bjoms.2021.08.006.
15. Zhao T, Yang H, Sui H, Salvi SS, Wang Y, Sun Y. Accuracy of a real-time, computerized, binocular, three-dimensional trajectory-tracking device for recording functional mandibular movements. PLoS One 2016;11:e0163934.
16. Corbett NE, DeVincenzo JP, Huffer RA, Shryock EF. The relation of the condylar path to the articular eminence in mandibular protrusion. Angle Orthod 1971;41:286–292.
17. Mack PJ. A computer analysis of condylar movement as determined by cuspal guidances. J Prosthet Dent 1989;61:628–633.
18. Lee WJ, Park KH, Kang YG, Kim SJ. Automated real-time evaluation of condylar movement in relation to three-dimensional craniofacial and temporomandibular morphometry in patients with facial asymmetry. Sensors (Basel) 2021;21:2591.
19. Koolstra JH, Naeije M, van Eijden TM. The three-dimensional active envelope of jaw border movement and its determinants. J Dent Res 2001;80:1908–1912.
20. Elledge R, Mercuri LG, Attard A, Green J, Speculand B. Review of emerging temporomandibular joint total joint replacement systems. Br J Oral Maxillofac Surg 2019;57:722–728.
21. Gakhal MK, Gupta B, Sidebottom AJ. Analysis of outcomes after revision replacement of failed total temporomandibular joint prostheses. Br J Oral Maxillofac Surg 2020;58:220–224.

22. Zheng J, Chen X, Jiang W, Zhang S, Chen M, Yang C. An innovative total temporomandibular joint prosthesis with customized design and 3D printing additive fabrication: a prospective clinical study. J Transl Med 2019;17:4.
23. Zou L, Zhao J, He D. Preliminary clinical study of Chinese standard alloplastic temporomandibular joint prosthesis. J Craniomaxillofac Surg 2019;47:602–606.
24. Ramos A, Mesnard M. Comparison of load transfers in TMJ replacement using a standard and a custom-made temporal component. J Craniomaxillofac Surg 2014;42:1766–1772.
25. Xu X, Luo D, Guo C, Rong Q. A custom-made temporomandibular joint prosthesis for fabrication by selective laser melting: Finite element analysis. Med Eng Phys 2017;46:1–11.